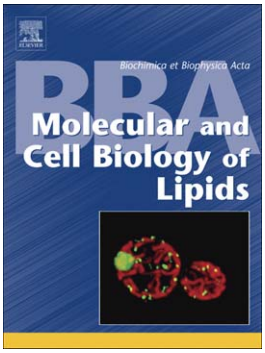

G protein-membrane interactions I: Gαi_1 myristoyl and palmitoyl modifications in protein-lipid interactions and its implications in membrane microdomain localization

Rafael Álvarez, David J. López, Jesús Casas, Victoria Lladó, Mónica Higuera, Tünde Nagy, Miquel Barceló, Xavier Busquets, Pablo V. Escribá

PII: S1388-1981(15)00147-X
DOI: doi: 10.1016/j.bbalip.2015.08.001
Reference: BBAMCB 57816

To appear in: *BBA - Molecular and Cell Biology of Lipids*

Received date: 5 April 2015
Revised date: 10 July 2015
Accepted date: 3 August 2015

Please cite this article as: Rafael Álvarez, David J. López, Jesús Casas, Victoria Lladó, Mónica Higuera, Tünde Nagy, Miquel Barceló, Xavier Busquets, Pablo V. Escribá, G protein-membrane interactions I: Gαi_1 myristoyl and palmitoyl modifications in protein-lipid interactions and its implications in membrane microdomain localization, *BBA - Molecular and Cell Biology of Lipids* (2015), doi: 10.1016/j.bbalip.2015.08.001

G protein-membrane interactions I: Gαi$_1$ myristoyl and palmitoyl modifications in protein-lipid interactions and its implications in membrane microdomain localization

Rafael Álvarez[a], David J. López[a], Jesús Casas[a], Victoria Lladó[a], Mónica Higuera[a], Tünde Nagy[a], Miquel Barceló[b], Xavier Busquets[a] and Pablo V. Escribá[a, *]

[a]Laboratory of Molecular Cell Biomedicine, Department of Biology, IUNICS, University of Islas Baleares, Carretera de Valldemossa km 7.5, E-07122 Palma de Mallorca, Spain.

[b]Bioinorganic and Bioorganic Research Group, Department of Chemistry, IUNICS, University of Islas Baleares, Carretera de Valldemossa km 7.5, E-07122 Palma de Mallorca, Spain.

[*] Corresponding Author at: Laboratory of Molecular Cell Biomedicine, Department of Biology, University of the Balearic Islands, Crta. Valldemossa km. 7.5, 07122, Palma (Spain). Tel.: +34-97117 33 31; Fax +34-971 17 31 84.
E-mail address: pablo.escriba@uib (Pablo V. Escribá).

Key words: G protein-lipid interactions; membrane microdomain; lipid structure; myristoylation; palmitoylation; cell signaling.

Abbreviations used: AcNPV, *Autographa californica* nuclear polyhedrosis virus; AMF, 30 μM $AlCl_3$, 50 mM $MgCl_2$ and 10 mM NaF; Biotin-HPDP, N-[6-(biotinamido)hexyl]-3'-(2'-pyridyldithio) propionamide; $C_{12}E_{10}$, polyoxyethylene 10-lauryl ether; CHO, cholesterol; GPCR, G protein-coupled receptor; FPA, 2-fluoropalmitic acid; HMA, 2-hydroxymyristic acid; λ_{ex}, excitation wavelength; λ_{em}, emission wavelength; Ld, liquid-disordered lamellar phase; Lo, liquid-ordered lamellar phase; LUV, large unilamellar vesicle; Myr, myristic acid; Pal, palmitic acid; Ni-NTA, nickel-nitrilotriacetic acid; NMT, myristoyl-CoA:protein N-myristoyltransferase; PC, phosphatidylcholine; PE, phosphatidylethanolamine; PS, phosphatidylserine; SM, sphingomyelin; TLCK, N-α-p-tosyl-L-lysine chloromethyl ketone; TPCK, L-1-tosylamido-2-phenyletyl chloromethyl ketone.

ABSTRACT

G proteins are fundamental elements in signal transduction involved in key cell responses, and their interactions with cell membrane lipids are critical events whose nature is not fully understood. Here, we have studied how the presence of myristic and palmitic acid moieties affects the interaction of the Gαi$_1$ protein with model and biological membranes. For this purpose, we quantified the binding of purified Gαi$_1$ protein and Gαi$_1$ protein acylation mutants to model membranes, with lipid compositions that resemble different membrane microdomains. We observed that myristic and palmitic acids not only act as membrane anchors but also regulate Gαi$_1$ subunit interaction with lipids characteristics of certain membrane microdomains. Thus, when the Gαi$_1$ subunit contains both fatty acids it prefers raft-like lamellar membranes, with a high sphingomyelin and cholesterol content and little phosphatidylserine and phosphatidylethanolamine. By contrast, the myristoylated and non-palmitoylated Gαi$_1$ subunit prefers other types of ordered lipid microdomains with higher phosphatidylserine content. These results in part explain the mobility of Gαi$_1$ protein upon reversible palmitoylation to meet one or another type of signaling protein partner. These results also serve as an example of how membrane lipid alterations can change membrane signaling or how membrane lipid therapy can regulate the cell's physiology.

1. INTRODUCTION

G proteins transduce signals from G protein-coupled receptors (GPCRs) to a variety of effector proteins that regulate the cytoplasmic concentrations of second messengers (e.g., cAMP, cGMP, DAG, Ca^{2+}, etc.) [1,2]. G proteins are composed of three subunits, an α, β and γ, and they interact with the cytoplasmic loops of GPCRs [1,3]. Agonist mediated activation of a GPCR induces the successive activation of several heterotrimeric G protein molecules, whose Gα subunit dissociates from Gβγ dimer. Subsequently, both molecular entities are directed towards their respective effector proteins [1], which might be localized to membrane microdomains with different lipid composition. Indeed, while the Gβγ dimers may remain near to the receptors where they can modulate other effectors or bind to the GRKs that phosphorylate GPCRs, the Gα monomers can move to different membrane microdomains in order to regulate effectors localized to different membrane microdomains [4].

At present, very little is known about the molecular bases underlying the interaction of the distinct G proteins subunits and forms (monomers, dimers and trimers) with the major membrane lipids that delineate membrane microdomains, such as phosphatidylcholine (PC), phosphatidylserine (PS), sphingomyelin (SM), phosphatidylethanolamine (PE), cholesterol (CHO), etc. The different Gα proteins and Gβγ dimers can be modified by the co/post-translational addition (reversible and irreversible) of lipids, events that are critical to localization, activity and, therefore, signal transduction [5-7]. This study assessed the role of the N-terminal fatty acyl moieties in the interaction of the Gαi$_1$ subunit with different membrane lipid microdomains. For this purpose, we examined the binding of purified wild type and mutant Gαi$_1$ proteins that lack one or two fatty acyl moieties to model membranes with distinct lipid compositions that resemble different membrane microdomains.

Biological membranes are fluid bilayers with dynamic microdomains that are rich in certain types of lipids and that have a heterogenous distribution of the different lipid species they contain [8-11]. In these microdomains, signaling proteins physically interact to propagate messages and as such, the membrane's lipid composition can regulate the signals within the cell and alterations in these domains may be linked to important diseases. In this context, G proteins are peripheral proteins whose different subunits exhibit preferences for lipid domains with distinct compositions and structures [10]. In their inactive state, G protein heterotrimers prefer membrane regions with a high PE content, a phospholipid whose effects in membrane curvature, fluidity, surface packing, hydration and fatty acyl composition, are different from those induced by PC. Upon receptor-mediated activation, the Gβγ dimer can remain in PE-

rich membrane domains while the Gα monomer prefers lamellar regions with a higher phosphatidylcholine (PC) content, where it coincides with effectors that are activated by this protein [4,10]. In this context, both fatty acyl moieties regulate the binding of Gαi$_1$ subunits to membrane with different content in PE and PS, which are the most abundant phospholipids at the cytoplasmic leaflet of the plasma membrane [12].

2. MATERIALS AND METHODS

2.1. Materials

The pFastBac 1 was purchased from Invitrogen (Barcelona, Spain). *Eco*RI and *Not*I restriction enzymes were from Fermentas (Madrid, Spain). Shrimp alkaline phosphatase was obtained from USB Corporation (Staufen, Germany). The Miller's LB Broth culture medium and agarose D-1 were from Conda Laboratories (Barcelona, Spain), while Grace's medium was from GIBCO (Madrid, Spain). Penicillin and streptomycin were from PAA (Pasching, Austria). The anti-Gαi$_1$ (clone R4) was from Santa Cruz Biotechnology (Santa Cruz, CA, USA). IRDye 800CW-linked donkey anti-mouse IgG and IRDye 680LT-linked streptavidin were provided by Li-Cor Biosciences (Madrid, Spain). Palmitoyl-CoA, egg-PC, liver-PE, egg-SM, brain-PS and CHO were obtained from Avanti Polar Lipids (Alabaster, AL, USA), and FPA from Biomol International (Lausane, Switzerland).

2.2. Cloning and site-directed mutagenesis of the Gαi$_1$ subunit

The cDNA encoding the recombinant rat Gαi$_1$ protein in pQE-60 (3.4 kb) was kindly provided by Prof. Alfred G. Gilman [13]. This protein contains an internal His tag (Table 1) and it was transferred into the pFastBac 1 eukaryotic expression vector after digestion with *Eco*RI and *Not*I. Mutants in the N-terminal region of the protein were generated by PCR amplification using primers that contained the selected mutations (Table 2). The resulting cDNA sequences were resolved by electrophoresis in 1% (w/v) agarose gels in 1 x TBE buffer (90 mM Tris-Borate, 2 mM EDTA) and recovered using a DNA Gel Extraction kit (Millipore) according to the manufacturer´s protocol. The amplified DNA (ca. 1 μg) was digested simultaneously for 90 minutes at 37ºC with *Eco*RI and *Not*I (0.5 units/μl of each enzyme) in 30 μl of 50 mM Tris-HCl buffer (pH 7.5), containing 10 mM $MgCl_2$, 100 mM NaCl and 0.1 mg/ml BSA. pFastBac 1 was digested under the same experimental conditions in a volume of 70 μl (0.3 units/μl of each restriction enzyme). After the enzymatic digestion, the vector was dephosphorylated for 90 minutes at 37ºC with alkaline phosphatase (0.2 units/μl) in 10 mM Tris-HCl buffer (pH 7.5) containing 10 mM $MgCl_2$ and 0.1 mg/ml BSA and purified by electrophoresis on a 0.5% (w/v) agarose gel. The vector and the Gαi$_1$ cDNA were combined at a 1:3 molar ratio and ligated using the DNA rapid ligation kit (Fermentas). Briefly, 50 ng of plasmid and 30 ng of amplified cDNA were combined with T4 DNA Ligase (0.3 units/µl) in a total volume of 25 μl 40 mM Tris-HCl buffer (pH 7.8) containing 10 mM $MgCl_2$, 10 mM DTT and 0.5 mM ATP, and this reaction was left for 1 hour at 25ºC.

2.3. Bacterial transformation

E. coli XL1-blue colonies transformed with the recombinant plasmids were selected and stored at -80ºC in Miller´s LB Broth medium supplemented with ampicillin (100 μg/ml), and finally mixed with an identical volume of 80% glycerol (v/v). The plasmids were purified by alkaline lysis (SDS 1%, NaOH 0.2 N) followed by isopropanol precipitation [14], and the resulting DNA pellet was washed with 1 ml ice-cold 70% ethanol, centrifuged and suspended in deionized water.

2.4. G protein expression in Sf9 cells

The recombinant proteins were expressed in Sf9 cells using the Bac-to-Bac Baculovirus Expression System (Invitrogen) [15]. For this purpose, the pFastBac 1 recombinant plasmid was introduced into *E. coli* DH10Bac competent cells, where it was transformed into a bacmid (AcNPV viral shuttle vector) by site-specific transposition. These bacteria were grown on selective Miller´s LB Broth containing 5-bromo-3-indolyl β-D-galactopyranoside (100 μg/ml, Bluo-Gal), isopropyl β-D-1-thiogalactopyranoside (40 μg/ml, IPTG), gentamicin (7 μg/ml), kanamycin (50 μg/ml) and tetracycline (10 μg/ml). White colonies were selected 72 hours after transformation, the recombinant bacmids generated were purified using the Plasmid Midi kit (Qiagen) and Sf9 cells were then transfected with these using Cellfectin (Invitrogen). After 96 hours, recombinant baculoviruses were collected and the positive viral clones were confirmed by immunoblotting.

2.5. Gαi$_1$ protein purification

Recombinant Gαi$_1$ proteins were produced in Sf9 cells and purified as described elsewhere [16]. For this purpose, Sf9 cells were cultured in suspension in Grace´s medium supplemented with 10% FCS (v/v), penicillin (100 units/ml) and streptomycin (100 μg/ml).

The *WT* and *Pal*$^-$ Gαi$_1$ subunits were purified from Sf9 cell membrane fractions [16] after harvesting Sf9 cells by centrifugation and suspending them in 15 ml of ice-cold 20 mM HEPES buffer (pH 8.0) containing β-mercaptoethanol (10 mM), NaCl (100 mM), $MgCl_2$ (1 mM), GDP (10 μM) and proteinase inhibitors (lysis buffer). The nuclei and unbroken cells were removed by centrifugation at 3,000 *g* for 10 minutes at 4ºC, and the resulting sample was centrifuged again at 100,000 *g* for 1 hour at 4ºC. The membranes recovered were suspended in 6 ml of HEPES buffer (50 mM, pH 8.0) containing β-mercaptoethanol (10 mM), NaCl (500 mM), CHAPS (16 mM), GDP (10 μM) and proteinase inhibitors, and after incubating for 1 hour with gentle shaking, the membranes were centrifuged at 100,000 *g* for 1

hour. The resulting supernatant (membrane extract) was dialyzed against HEPES buffer supplemented with GDP (0.5 μM) and leupeptin (50 ng/ml), and then purified by chromatography on a Ni-NTA column (1 ml of resin, Invitrogen). Subsequently, the resin was washed with 30 ml of HEPES buffer (20 mM, pH 8.0), containing β-mercaptoethanol (10 mM), NaCl (400 mM), $C_{12}E_{10}$ (0.05%, v/v), GDP (10 μM), leupeptin (0.5 μg/ml), imidazole (15 mM), using an increasing and discontinuous thermal gradient (4, 17 and 25ºC) [17]. The column was then washed with 20 ml of HEPES buffer (20 mM, pH 8.0), containing $MgCl_2$ (0.5 mM), β-mercaptoethanol (10 mM), NaCl (100 mM), $C_{12}E_{10}$ (0.05%, v/v), GDP (10 μM), leupeptin (0.5 μg/ml), imidazole (15 mM) at 30 ºC, and it was then activated with 10 ml of HEPES buffer (20 mM, pH 8.0) containing $AlCl_3$ (30 μM), $MgCl_2$ (50 mM) and NaF (10 mM, AMF buffer). Finally, the Gαi$_1$ protein was eluted with HEPES buffer (20 mM, pH 8.0) containing β-mercaptoethanol (10 mM), NaCl (100 mM), $MgCl_2$ (1 mM, elution buffer) [16] and supplemented with a step gradient of imidazole (40, 80, 120, 240 and 300 mM). The purified protein was dialyzed and stored at -80ºC until use. The *Myr*$^-$ Gαi$_1$ mutant protein (Table 2) was overexpressed and purified from the cytosolic fraction of infected Sf9 cells, which had been harvested and suspended in 5 ml of ice-cold lysis buffer as indicated above. The *Myr*$^-$ Gαi$_1$ protein was purified from the supernatant by affinity chromatography as indicated above and fractionated by SDS-PAGE followed by coomassie blue staining (Figure 2A) as described elsewhere [18].

2.6. Gαi$_1$ protein acylation

To detect *in vivo* acylation, 16 h after baculoviral inoculation, of Sf9 cells (3 x 10^6) were incubated for 32 h with the acylation inhibitors, 2-hydroxymyristic acid (45 μM, for myristoylation analysis) and 2-fluoropalmitic acid (30 μM, for palmitoylation analysis). The cells were centrifuged twice at 600 *g* and 4ºC for 5 min and suspended in extraction buffer (10 mM Tris-Cl, 50 mM NaCl, 1 mM $MgCl_2$, 2 mM EDTA, pH 7.4). The pellets were finally suspended in 300 μl of extraction buffer supplemented with 1% SDS (v/v) and protease inhibitors as indicated above. The cells were disrupted by ultrasound using a Branson probe-type sonicator (Danbury, CT). Proteins were detected in immunoblots (see below), using a myristoylated and non-myristoylated *WT* Gαi$_1$ protein as standards.

Purified myristoylated *WT* Gαi$_1$ protein was further palmitoylated by incubating 0.1-0.3 nmol of protein with 20 nmol of palmitoyl-CoA for 3 hours at 30ºC in 1 ml of 20 mM HEPES buffer containing 2 mM $MgCl_2$, 50 mM NaCl, 1 mM EDTA, 0.2 mM DTT, 0.5 μM GDP and

7.5 mM CHAPS (pH 7.6) [19]. The palmitoylated *WT* Gαi$_1$ protein was then dialyzed against dialysis buffer (20 mM HEPES buffer, pH 8.0) containing 3 mM $MgCl_2$, 0.2 mM DTT, 100 mM NaCl, 1 mM EDTA, 0.5 μM GDP and 50 ng/ml leupeptin.

Autoacylation of *WT* Gαi$_1$ protein was assessed by acyl-biotinyl exchange [20]. To block the free thiol moieties, 600 ng of recombinant Gαi$_1$ protein was incubated with 0.1% S-methyl methanethiosulfonate for 20 minutes at 50°C in 250 mM Hepes buffer [pH 8.0] containing 1 mM EDTA and 2.5 mM SDS, and it was then dialyzed against phosphate-buffered saline (PBS) containing 1 mM EDTA. Then, recombinant proteins were treated with 1 M hydroxylamine [pH 7.4] and dialyzed. This protein suspension was then mixed with 0.2 mM biotin-HPDP for 1 hour at room temperature and analyzed by non-denaturing immunoblotting, as described below. Biotinylated protein was incubated with streptavidin conjugated to a near infrared dye (IRDye^{TM} 680LT Streptavidin) and the infrared signal was subsequently detected with an ODISSEY near infrared radiation detection system.

2.7. Gαi$_1$ protein binding to biological membranes

These Sf9 cells were harvested 48 hours after infection with recombinant baculovirus encoding the *WT* or mutant Gαi$_1$ proteins and centrifuged at 600 *g* for 5 minutes at 25ºC. The cells were suspended and re-centrifuged in buffer K (20 mM HEPES [pH 8.0], 1 mM $MgCl_2$, 100 mM KCl), and they were then resuspended in 1 ml of buffer K supplemented with 20 μM GTP and proteinase inhibitors, before they were subjected to sonication (6 10-s pulses at 10% amplitude and 10 s between pulses). The homogenate was centrifuged at 1,000 *g* for 10 minutes at 25ºC to remove the nuclei and unbroken cells, and the supernatant was then centrifuged at 100,000 *g* for 1 h at 25ºC. The resulting pellet was resuspended in the same initial volume (1 ml) and homogenized in a Potter-Elvehjem homogenizer.

2.8. Gαi$_1$ protein binding to model membranes

Model membranes (liposomes) were prepared from 30 mM stock solutions of natural lipids (PC, PE, PS, CHO and SM in chloroform/methanol, 2/1 [v/v]) by mixing the appropriate volumes of each in glass vials. The solvent was then removed under argon and the lipid film was submitted to vacuum for 2 hours to remove the traces of solvent. Subsequently, the lipid films were resuspended with vigorous vortexing in 20 mM Tris-HCl, 100 mM KCl, 0.1 mM EDTA at pH 7.4, obtaining a final concentration of 3 mM (lipid phosphorus). These multilamellar vesicles (MLVs) were submitted to ten freeze/thaw cycles (-196ºC/42ºC) and subsequently, the different lipid emulsions were passed 11 times through a 400 nm pore

polycarbonate membrane to generate LUVs [21] using a mini-extruder (Avanti Polar Lipids). The lipid phosphorux concentration was determined as described [22].

Liposomes (1 mM) were incubated for 1 hour at 25ºC with 150 ng of purified Gαi$_1$ protein in the presence of 50 μM GTPγS and in a total volume of 300 μl. Unbound G proteins were then separated from the membrane-bound G proteins by centrifugation at 90,000 *g* for 1 hour at 25ºC. Finally, the membrane pellets were resuspended in 36 μl of 80 mM Tris-HCl buffer [pH 6.8], containing 4% SDS, and mixed with 4 μl of 10x electrophoresis loading buffer (120 mM Tris HCl [pH 6.8], 1.43 M β-mercaptoethanol, 2% SDS and 50% glycerol).

2.9. G protein binding quantification

To quantify the wild type and mutant Gαi$_1$ proteins bound to biological and model membranes, they were fractionated on 10% polyacrylamide gels and then transferred to nitrocellulose membranes as described elsewhere [23]. These membranes were incubated with anti-Gαi$_1$ (1:400 dilution) first, followed by incubation with IRDye 800CW-linked donkey anti-mouse IgG (1:4,000 dilution). IRDye 680LT-linked streptavidin (diluted 1:5,000) was used to detect the biotinylated Gαi$_1$-protein in acyl-biotinyl exchange experiments. In these assays, a 1:600 dilution of anti-Gαi$_1$ was used to detect the total Gαi$_1$ protein in the immunoblots and antibody binding was detected by near infrared fluorescence using an ODISSEY near infrared radiation detection system (LI-COR Biosciences). The excitation and emission wavelengths (λ_{ex} and λ_{em}) for the IRDye 800CW-linked IgGs were 778 nm and 795 nm, respectively, and those for IRDye 680LT-linked streptavidin were 676 nm and 694 nm, respectively.

To quantify the Gαi protein, samples were evaluated using standard curves (i.e., a plot of the Gαi protein loaded against the integrated optical density [IOD] of the immunoreactive bands), consisting of four points of different protein content prepared from a commercial Gαi$_1$ protein batch (Calbiochem). The binding to liposomes containing different phospholipid mixtures was then normalized to the binding to pure PC liposomes, which was considered as 100%.

2.10. G protein structure analysis

The analyzed protein sequences were obtained from the protein database record at the National Center for Biotechnology Information (http://www.ncbi.nlm.nih.gov). The sequence identification numbers assigned by the International Nucleotide Sequence Database Collaboration to the different myristoylated Gα proteins shown were: EDL81916.1 (Gαi$_3$),

P63096.2 (Gαi$_1$), P04899.3 (Gαi$_2$), NP_037321.1 (Gαz), NP_059023.1 (Gαo), P29348.3 (Gαt$_3$), NP_001102250.2 (Gαt). The secondary structure prediction of the N-terminal region of these Gα proteins was performed on the *Psi-Pred* server using default parameter settings [24]. The N-terminal sequences of the proteins mentioned above were aligned with the *CLUSTAL W (1.81)* tool on the *Biology WorkBench Interface (v. 3.2)*. A bi-dimensional projection of the N-terminal α helix of the Gαi$_1$ protein was obtained with the *HELIQUEST* server [25]. In this projection the one-letter code size was proportional to amino acid volume. The effect of the lipid chains on the N-terminus of Gαi was assessed by *molecular mechanics* calculations, using the *MMFF94* force field, of the first 5 amino acids of the *Myr*$^-$, *Pal*$^-$ and *Pal*$^+$ Gαi$_1$ proteins. The starting point for each minimization was the 2D representation of the desired moiety. The theoretical study was carried out using *ChemBio 3D Ultra 12.0* software from Perkin Elmer (formerly CambridgeSoft). The Cartesian coordinates of the 3 different C-terminal regions of the various G protein constructs are included as supporting information (Tables S1-S3 and pbd files). Structural alignment of the three modelled peptides was done with the *Discovery Studio 3.0* software. Acylated peptides were aligned each other by the myristaoyl moiety and by the N-terminal carbon atom, whereas the non-acylated peptide was aligned with the other two peptides only by the N-terminal carbon atom.

A multiple sequence alignment of different Gα proteins was carried out using the *CLUSTAL W (1.81)* software, while the secondary structure prediction of the N-terminal region of Gαi$_1$ was performed on the *Psi-Pred* server [24]. A bi-dimensional projection of the N-terminal α helix of the Gαi$_1$ protein was obtained with the *HELIQUEST* server [25]. The effect of the lipid chains on the N-terminus of Gαi was assessed by *MMFF94 molecular mechanics* of the first 5 amino acids of the *Myr*$^-$, *Pal*$^-$ and *Pal*$^+$ Gαi$_1$ proteins. This study was carried out using *ChemBio 3D Ultra 12.0* software from Perkin Elmer (formerly CambridgeSoft).

2.11. Data Analysis

Origin software was used for data analysis and statistics. Unless otherwise indicated the results were expressed as the mean ± SEM from the number of experiments indicated (n). To determine statistical significance, *ANOVA* or an unpaired 2-sample *t* test were used when appropriate. Differences were considered statistically significant at $p<0.05$.

3. **RESULTS**

3.1. Purification and Characterization of Recombinant Gαi$_1$ Proteins

Cells overexpressing *WT* and *Pal*$^-$ Gαi$_1$ proteins, both susceptible to be myristoylated, were incubated with 2-hydroxymyristic acid (HMA), which is converted to the potent inhibitor of the myristoyl-CoA:protein N-myristoyltransferase (NMT), 2-hydroxymyristoyl-CoA [26]. As a consequence of this treatment, non-myristoylated *WT* and *Pal*$^-$ Gαi$_1$ proteins were obtained. These proteins lacking myristic acid had a slightly slower electrophoretic mobility than the myristoylated *WT* and *Pal*$^-$ Gαi$_1$ proteins overexpressed in the absence of HMA, and their electrophoretic behavior was similar to that of the *Myr*$^-$ Gαi$_1$ mutant protein (Figure 1A). Indeed, this phenomenon was used to determine the presence or absence of myristic acid in the *WT* and *Myr*$^-$ Gαi$_1$ proteins (Figure 1B and refs. 4, 27). By contrast, and as described previously [28], an inhibitor of palmitoylation, 2-fluoropalmitic acid, did not affect either protein myristoylation or the electrophoretic mobility of the *WT* Gαi$_1$ subunit (Figure 1A).

Palmitoylation of Gαi$_1$ was demonstrated by Cys-3 biotinylation, which only occurs if palmitic acid is previously bound to this amino acid. As expected, no biotinylation of the *Pal*$^-$ Gαi$_1$ protein was detected, reflecting the absence of palmitic acid. By contrast, an intense band was observed for Pal$^+$ *WT* Gαi$_1$ protein (Figure 1C), demonstrating its palmitoylation at Cys-3.

3.2. Gαi$_1$ acylation is critical for its preference for lamellar-prone microdomains

In the present study, four types of Gαi$_1$ proteins with different degrees of acylation were produced. Three types of myristoylated Gαi$_1$ proteins were generated: a non-palmitoylated *Pal*$^-$ Gαi$_1$ protein; and two types of *WT* Gαi$_1$ proteins with different extents of palmitoylation, *WT* Gαi$_1$ and *Pal*$^+$ Gαi$_1$, respectively, the latter being the same as the wild type but submitted to additional *in vitro* palmitoylation (see Experimental Procedures). The lack of the N-terminal myristic acid moiety in the *Myr*$^-$ Gαi$_1$ mutant protein also prevented the palmitoylation of this protein and thus, the *Myr*$^-$ *Pal*$^-$ Gαi$_1$ mutant was not produced. *However, the Myr*$^-$ mutant should be considered a *Myr*$^-$ *Pal*$^-$ Gαi$_1$ form. We analyzed the binding of these Gαi$_1$ proteins to different model membranes, each of which resembled distinct membrane microdomains. In this context, vesicles composed of PC form uniform lamellar structures that resemble the bulk of the plasma membrane, whereas PE is critical in the formation of disordered membrane (L_d) domains with a high non-lamellar-phase

propensity (negative curvature strain) [4, 10, 29]. In addition, these PE-rich domains have a lower surface packing strain, less hydration and fluidity than PC-rich domains. In all cases, myristoylated Gαi$_1$ protein bound less to model membranes with higher PE content (25ºC) and as the concentration of PE increased in the membranes, the fully acylated *Pal*$^+$ *WT* Gαi$_1$ protein showed the strongest decrease in membrane binding (Figures 2A and 2B). *WT* Gαi$_1$ and *Pal*$^-$ Gαi$_1$ proteins also associated less with membranes as their PE concentration increased, although the reduction in binding was not as marked as for the *Pal*$^+$ *WT* Gαi$_1$ protein (Figures 2A and 2C). On the other hand, the absence of myristoylation almost completely abolished Gαi$_1$ protein binding to lipid vesicles (Figure 2A). However, no significant differences were observed in the binding of *Myr*$^-$ Gαi$_1$ to model membranes with increasing PE content (Figure 2C).

Similarly, model PC membranes containing the nonlamellar-prone lipid, diacylglycerol (DAG), showed decreased *Pal*$^+$ *WT* Gαi$_1$ protein binding compared to lamellar-prone PC vesicles (4.4±0.9 and 9.1±3.8 for membranes containing 5 mol% and 10 mol% DAG, respectively).

3.3 Palmitoylation reduces myristoylated Gαi$_1$ protein binding to PS-rich membranes

Myristoylated and palmitoylated (*Pal*$^+$ *WT*) Gαi$_1$ proteins had less affinity for membranes with a high PS content (Figure 3). In this context, the binding of the non-myristoylated Gαi$_1$ protein (*Myr*$^-$) to PS vesicles did not change significantly as the PS content increased, although the amount of protein bound was very low in all cases (Figure 3B). By contrast, the binding of myristoylated and not palmitoylated *Pal*$^-$ Gαi$_1$ protein to lipid membranes containing 40 mol% PS was markedly and significantly greater than that to PC membranes. This indicates that myristoylated but not palmitoylated Gαi$_1$ proteins prefer negatively charged and lamellar-prone microdomains (Figure 3). Because palmitoylation is a reversible acylation process that depends of the cell's signaling status and PS is a phospholipid abundant at certain membrane microdomains, these results help understand how Gαi$_1$ protein may move at the membrane surface to receive or propagate cell signals.

3.4. Binding of Gαi$_1$ to lipid-raft-like (L$_o$) membranes increases with the degree of acylation

The dual acylated Pal$^+$ WT Gαi$_1$ protein bound more to highly lamellar-prone membranes composed of PC (L$_d$ phase) or PC:PE:CHO:SM (1:1:1:1, molar ratio; L$_o$ + L$_d$ phases) than the partially palmitoylated *WT* Gαi$_1$ protein. Moreover, less acylation (Myr$^-$ Gαi$_1$, which lacks

myristic and palmitic acids) resulted in a drastic decrease in Gαi$_1$ protein binding to these model membranes (Figure 4).

3.5. Effect of lipid acylation on Gαi$_1$ protein binding to cell membranes

As described elsewhere [5], the presence of myristic acid in Gαi$_1$ proteins is critical for its interaction with Sf9 cell membranes (Figure 5). The differences between *WT* Gαi$_1$ and *Pal*$^-$ Gαi$_1$ in terms of binding to biological membranes were not significant, further suggesting that myristic acid drives the interaction between this protein and Sf9 cell membranes. Finally, the *Myr*$^-$ Gαi$_1$ protein bound less to Sf9 cell membranes than the other forms, which supports the importance of myristic acid in binding to biological membranes and further supports that palmitic acid influences mobilization between membrane microdomains [30, 31].

3.6. Gαi$_1$ structure modification by palmitoylation and membrane binding

The amino-terminal region of the Gαi$_1$ protein was studied by computer-assisted sequence alignment and the predicted secondary (α-helical) structure was simulated close to the myristoylation site (Figure 6, Figure S1, Tables S1, S2, S3). The data obtained was consistent with previous studies [32, 33], with the multiple-sequence alignment of myristoylated Gα proteins demonstrating that this α–helix was a conserved structural motif (Figure 6B). Furthermore, several conserved basic amino acids were concentrated on one side of the α–helix, giving rise to a region with a high positive charge density, as shown in the helical projection (Figure 6C, blue circles). This cluster of key basic amino acids seems to play a very important role in the Gαi$_1$ protein-lipid interactions, which was confirmed by its binding to membranes with a net negative charge (i.e., with PS). Finally, the presence of palmitic acid changes the overall structure of the Gαi$_1$ protein N-terminal region, changing the membrane contact surface of the α–helix from the positively charged amino acid face to a more neutral area (Figure 6D, Figure S1). The first 5 amino acids in the Gαi$_1$ protein form a random coil structure with high mobility that allows a conformational change, exposing both fatty acyl moieties to the neutral side of the N-terminal α-helix. Therefore, palmitoylation is relevant for Gαi$_1$ protein-membrane interactions, as evident in the binding assays to liposomes that mimic different types of membrane microdomain.

4. DISCUSSION

Various studies have investigated the interaction between G proteins and membranes [32-37]. However, most studies focused on the protein, considering the membrane an homogeneous hydrophobic target and disregarding the heterogeneous nature of membranes, which contain different types of structures and microdomains depending on their lipid composition [38]. Thus, it is well known that Gα protein fatty acyl (myristoyl or palmitoyl) moieties are necessary for its attachment to the membrane. However, the role of the G protein lipid modifications in their membrane lipid/microdomain preferences has received little attention. We previously showed that heterotrimeric G proteins prefer non-lamellar prone (PE-rich) rather than lamellar prone (PC-rich) membrane microdomains, whereas the isolated Gα subunit displays the opposite preference [10]. In the present study, we investigated the complex Gαi$_1$-membrane interactions [39] using wild type and mutated protein subunits with different degrees of acylation, and model membranes with different lipid compositions that resemble distinct biological membrane microdomains. The use of model membranes (large unilamellar/oligolamellar vesicles) allowed us investigate the affinity of this G protein monomer for lipid structures with varying composition of the major membrane lipids, a type of study that cannot be achieved in natural membranes due to the dynamic nature of membrane microdomains. In this context, irreversible Gαi$_1$ protein myristoylation is critical for membrane binding while palmitoylation, a reversible process whose relevance is only just starting to be understood [31, 40, 41], might be more important in determining the localization of the Gαi$_1$ subunit to different microdomains in membranes, as shown in the present study. Therefore, this event is crucial to GPCR-associated signaling because this protein most likely interacts with different effectors of signaling in the distinct membrane microdomains. Accordingly, the presence or absence of palmitic acid, although not normally critical for the membrane localization of Gαi$_1$ protein, may in part determine the type of signals propagated to the cell.

The most remarkable difference between heterotrimeric G proteins and the alpha monomer is the preference of the former for PE-rich microdomains and that of the latter for PC-rich microdomains [9, 10, 42]. PE-rich membrane regions show a high non-lamellar phase propensity, a less dense surface packing, and lesser hydration (among other biophysical properties) compared to PC, which could justify the opposite behavior observed for the interaction of monomeric or oligomeric G proteins with membranes. Here, we found that the higher the degree of palmitoylation, the greater the difference in affinity between lamellar-

and non-lamellar-prone lipid structures, whereas in the absence of palmitic acid little or no preference was evident. In this context, the PE concentrations used in these experiments resembled those of lamellar-prone domains (0 mol% PE), the average of the inner membrane leaflet (50 mol% PE) and PE-rich microdomains (80 mol% PE). Similarly, *Pal*$^+$ WT Gαi$_1$ showed less affinity for DAG-containing membranes. Both DAG and PE form non-lamellar prone microdomains, which exhibit a number of biophysical differential properties with respect to lamellar prone PC membranes. Because both types of lamellar prone model membranes used in this study have a dense surface packing, the present results suggest that insertion of Gαi$_1$ acyl moieties has a better binding to mebranes with high lateral surface pressure rather than membranes with low surface packing.

A relevant feature of the N-terminal region of the Gαi$_1$ subunit is the presence of several positively charged amino acids whose position with respect to the membrane differs in the presence or absence of palmitic acid (Figure 6). These amino acids have been associated with electrostatic interactions at the inner face of the membrane. Indeed, PS has a negative charge and it is more abundant at this cytoplasmic face. In this context, we observed greater binding of the Pal$^-$ Gαi$_1$ protein to model membranes containing PS. By contrast, the presence of palmitic acid (*Pal*$^+$ WT Gαi$_1$) significantly reduced the binding of the Gα subunit to membranes. This most likely happens because the N-terminal region of the Gαi$_1$ protein undergoes a conformational change upon palmitoylation that leaves the hydrophobic region rather than the positively charged side of the α-helix in contact with the membrane surface (Figure 6). These results further indicate that palmitic acid constitutes a switch for the localization of Gα subunits to different membrane microdomains, showing the importance of the N-terminal region of this protein in its interactions with the membrane [33, 43-45]. For these experiments, the proportions of PS used resembled that of the bulk of the membrane (10 mol%), the bulk of the inner membrane leaflet (20 mol%) and its possible abundance in PS-rich microdomains (40 mol%).

In the present study, we used model membranes containing PC:PE:CHO:SM (1:1:1:1, mol:mol) because they can generate raft-like microdomains (liquid ordered, L$_o$) and liquid disordered (L$_d$) phases [46]. The binding of the 4 Gαi$_1$ protein forms studied to this type of membranes was not significantly different to that to lamellar-prone PC membranes, further demonstrating that lamellar propensity is more important than order in Gαi$_1$ protein-lipid interactions. Interestingly, their binding to both types of lamellar-prone membranes increased with the degree of acylation, with the greatest binding corresponding to *Pal*$^+$ Gαi$_1$, followed by *WT* Gαi$_1$, *Pal*$^-$ Gαi$_1$ and *Myr*$^-$ Gαi$_1$. These results explain how dual acylation with

saturated fatty acids, as in Gαi$_1$, has been shown to induce the localization of the Gα subunit to lamellar-prone and raft-like membrane domains [10, 35, 47, 48].

The role of co- and post-translational modifications have been usually associated with G protein localization and activity but the differential interaction with membrane microdomains remains largely unknown (for a review about G protein subunit lipid modification see [49]). In this work, we also showed that the presence of myristic acid is critical for the localization of Gα subunits to Sf9 cell membranes, as described elsewhere [4, 49]. However, the lack of palmitic acid did not cause a significant decrease in myristoylated Gαi$_1$ protein binding to biological membranes. This further suggests that myristic acid is necessary for membrane targeting and palmitic acid is involved in Gαi$_1$ protein mobilization to certain microdomains [34, 50-52]. While palmitic acid alone might also target Gαi$_1$ protein to the membrane, this does not happen *in vivo* [19]. Indeed, other studies have suggested that palmitic acid is not crucial for the binding of inactive Gαq protein to membranes [53]. From the results obtained, we conclude that palmitic acid facilitates Gαi$_1$ protein localization to membrane microdomains with high lamellar propensity, preferably without negative charges (i.e., containing PC but not PS and PE). Considering that about two thirds of the phospholipids in the inner monolayer of the membrane are PS and PE species [12], the microdomains where the double acylated monomeric protein might be found could constitute only a small fraction of the membrane. In this context, the main molecular role of Gαi proteins is to inhibit the effector adenylyl cyclase, and both proteins have been localized to raft-like regions where they co-localize with caveolin and other raft markers, consistent with the results presented here [54, 55]. On the other hand, myristoylated but not palmitoylated Gαi protein would localize to lamellar-prone membrane domains with a net negative charge (PS-rich). Thus, both fatty acids appear to be responsible for the lamellar preference of the Gαi$_1$ monomer but they fulfill an opposing role in its electrostatic interactions with the membrane, most likely due to the conformational difference of the N-terminal region in the presence of certain fatty acids. Other lipid anchors, such as the isoprenyl moieties (present in Gγ protein, Ras, etc.), are branched and bigger than the aforementioned fatty acids and they cannot fit into lamellar-prone membrane regions, preferring membrane regions with a high non-lamellar propensity, with lower surface packing density [56]. Moreover, the present results are in agreement and in part explain the differential microdomain localization of Gαi depending on its acylation status [30,57]. In the latter study [57] was shown that G proteins exhibit a preference for certain membrane microdomains but they may also be present in other microdomains. In the present study, Gαi$_1$ protein localization to any type of membrane domain would correlate with the

presence of myristic acid, whereas palmitic acid would be involved in the preference of the transducer for lamellar-prone microdomains with low acidic (e.g., PS) phospholipid content. Moreover, because palmitoylation is reversible, the *in vivo* presence of Gαi$_1$ protein to various microdomains [57] might be justified by the differential membrane lipid preference of palmitoylated and non-palmitoylated forms of this protein. In this context, it is important to know how membrane lipids can regulate the cell's physiology, as well as how interventions aimed at regulating the membrane lipid composition can reverse altered cellular functions (membrane lipid therapy) [29, 55, 58]. The data presented here will certainly enhance our understanding of the influence of lipids and lipid modifications on protein-membrane interactions.

ACKNOWLEDGEMENTS We thank Dr. Alfred G. Gilman (University of Texas Southwestern Medical Center, Dallas) for the pQE-60 expression vector (3.4 kb) containing cDNA encoding the recombinant rat Gαi$_1$ protein. This work was supported by the grants BIO2010-21132 and BIO2013-49006 (Ministerio de Economía y Competitividad, Spain), Ajuts a Grups Competitius (Govern de les Illes Balears) and by the Marathon Foundation. R.A. was supported by Fellowships from the Programa de Formación de Unidades Asociadas al CSIC (Ministerio de Educación, Cultura y Deporte, Spain) and from the Marathon Foundation. D.J.L. and S.T. held contracts from the 'Torres Quevedo' Program (Ministerio de Economía y Competitividad, Spain). J.C. and T.N. were supported by Fellowships from the Ministerio de Educación, Cultura y Deporte (Spain). V.L. and M.H. were supported by Fellowships from the Marathon Foundation.

REFERENCES

[1] E.J. Neer, Heterotrimeric G proteins: organizers of transmembrane signals, Cell 80 (1995) 249-257.

[2] M. Faure, T.A. Voyno-Yasenetskaya, H.R. Bourne, cAMP and βγ Subunits of Heterotrimeric G proteins stimulate the mitogen-activated protein kinase pathway in COS-7 cells, J. Biol. Chem. 269 (1994) 7851-7854.

[3] B.K. Kobilka, G protein coupled receptor structure and activation, Biochim. Biophys. Acta 1768 (2007) 794-807.

[4] O. Vögler, J.M. Barceló, C. Ribas, P.V. Escribá, Membrane interactions of G proteins and other related proteins, Biochim. Biophys. Acta 1778 (2008) 1640-1652.

[5] T.L. Jones, W.F. Simonds, J.J. Merendino Jr., M.R. Brann, A.M. Spiegel Myristoylation of an inhibitory GTP-binding protein alpha subunit is essential for its membrane attachment, Proc. Natl. Acad. Sci. U.S.A. 87 (1990) 568-572.

[6] K.H. Muntz, P.C. Sternweis, A.G. Gilman, S.M. Mumby, Influence of gamma subunit prenylation on association of guanine nucleotide-binding regulatory proteins with membranes, Mol. Biol. Cell 3 (1992) 49-61.

[7] M.E. Linder, P. Middleton, J.R. Hepler, R. Taussig, A.G. Gilman, S.M. Mumby, Lipid modifications of G proteins: alpha subunits are palmitoylated, Proc. Natl. Acad. Sci. USA 90 (1993) 3675-3679.

[8] S.J. Singer, G.L. Nicolson, The fluid mosaic model of the structure of cell membranes, Science 175 (1972) 720-731.

[9] P.V. Escribá, A. Ozaita, C. Ribas, A. Miralles, E. Fodor, T. Farkas, J.A. García-Sevilla Role of lipid polymorphism in G protein-membrane interactions: nonlamellar-prone phospholipids and peripheral protein binding to membranes, Proc. Natl. Acad. Sci. U.S.A. 94 (1997) 11375-11380.

[10] O. Vögler, J. Casas, D. Capo, T. Nagy, G. Borchert, G. Martorell, P.V. Escribá, The Gβγ dimer drives the interaction of heterotrimeric Gi proteins with nonlamellar membrane structures, J. Biol. Chem. 279 (2004) 36540-36545.

[11] D. Lingwood, K. Simons, Lipid rafts as a membrane-organizing principle, Science 327 (2010) 46-50.

[12] J.E. Rothman, J. Lenard, Membrane asymmetry, Science 195 (1977) 743-753.

[13] R. Herrmann, M. Heck, P. Henklein, C. Kleuss, K.P. Hofmann, O.P. Ernst, Sequence of interactions in receptor-G protein coupling, J. Biol. Chem. 279 (2004) 24283-24290.

[14] J. Sambrook, D.W. Russell, Book Molecular Cloning: A Laboratory Manual, third ed., Cold Spring Harbor Laboratory, Cold Spring Harbor, New York, 2001.

[15] V.A. Luckow, S.C. Lee, G.F. Barry, P.O. Olins, Efficient generation of infectious recombinant baculoviruses by site-specific transposon-mediated insertion of foreign genes into a baculovirus genome propagated in Escherichia coli, J. Virol. 67 (1993) 4566-4579.

[16] T. Kozasa, A.G. Gilman, Purification of recombinant G proteins from Sf9 cells by hexahistidine tagging of associated subunits. Characterization of alpha 12 and inhibition of adenylyl cyclase by alpha z, J. Biol. Chem. 270 (1995) 1734-1741.

[17] C.R. Lowe, Laboratory Techniques in Biochemistry and Molecular Biology. An Introduction to Affinity Chromatography, first ed., Elsevier Biomedical Press, Amsterdam, The Netherlands, 1979.

[18] D.M. Watterson, W.G. Harrelson Jr., P.M. Keller, F. Sharief, T.C. Vanaman, Structural similarities between the Ca^{2+}-dependent regulatory proteins of 3':5'-cyclic nucleotide phosphodiesterase and actomyosin ATPase, J. Biol. Chem. 251 (1976) 4501-4513.

[19] J.A. Duncan, A.G. Gilman, Autoacylation of G protein alpha subunits, J. Biol. Chem. 271 (1996) 23594-23600.

[20] R.C. Drisdel, W.N. Green, Labeling and quantifying sites of protein palmitoylation, Biotechniques 36 (2004) 276-285.

[21] L.D. Mayer, M.J. Hope, P.R. Cullis, Vesicles of variable sizes produced by a rapid extrusion procedure, Biochim. Biophys. Acta. 858 (1986) 161-168.

[22] C.J.F. Böttcher, C.M. van Gent, C. Pries, A rapid and sensitive sub-micro phosphorus determination, Analytica Chimica Acta 24 (1961) 203-204.

[23] P.V. Escribá, M. Sastre, J.A. García-Sevilla, Increased density of guanine nucleotide-binding proteins in the postmortem brains of heroin addicts, Arch. Gen. Psychiatry 51 (1994) 494-501.

[24] D.T. Jones, Protein secondary structure prediction based on position-specific scoring matrices, J. Mol. Biol. 292 (1999) 195-202.

[25] R. Gautier, D. Douguet, B. Antonny, G. Drin, HELIQUEST: a web server to screen sequences with specific alpha-helical properties, Bioinformatics 24 (2008) 2101-2102.

[26] L.A. Paige, G.Q. Zheng, S.A. DeFrees, J.M. Cassady, R.L. Geahlen, Metabolic activation of 2-substituted derivatives of myristic acid to form potent inhibitors of myristoyl CoA:protein N-myristoyltransferase, Biochemistry 29 (1990) 10566-10573.

[27] P. Chan, M. Gabay, F.A. Wright, W. Kan, S.S. Oner, S.M. Lanier, A.V. Smrcka, J.B. Blumer, G.G. Tall Purification of Heterotrimeric G Protein α Subunits by GST-Ric-8 Association, J. Biol. Chem. 286 (2011) 2625-2635.

[28] T.L. Jones, M.Y. Degtyarev, P.S. Backlund Jr., The stoichiometry of G alpha(s) palmitoylation in its basal and activated states, Biochemistry 36 (1997) 7185-7191.

[29] P.V. Escribá, Membrane-lipid therapy: a new approach in molecular medicine, Trends Mol. Med. 12 (2006) 34-43.

[30] C. Huang, J.A. Duncan, A.G. Gilman, S.M. Mumby, Persistent membrane association of activated and depalmitoylated G protein alpha subunits, Proc. Natl. Acad. Sci. U.S.A. 96 (1999) 412-417.

[31] M.J. Bijlmakers, M. Marsh, The on-off story of protein palmitoylation, Trends Cell Biol. 13 (2003) 32-42.

[32] M.A. Wall, D.E. Coleman, E. Lee, J.A. Iniguez-Lluhi, B.A. Posner, A.G. Gilman, S.R. Sprang, The structure of the G protein heterotrimer Gi alpha 1 beta 1 gamma 2, Cell 83 (1995) 1047-1058.

[33] M. Kosloff, N. Elia, Z. Selinger, Structural homology discloses a bifunctional structural motif at the N-termini of G alpha proteins, Biochemistry 41 (2002) 14518-14523.

[34] C.S. Fishburn, P. Herzmark, J. Morales, H.R. Bourne Gbetagamma and palmitate target newly synthesized Galphaz to the plasma membrane, J. Biol. Chem. 274 (1999) 18793-18800.

[35] S. Moffett, D.A. Brown, M.E. Linder, Lipid-dependent targeting of G proteins into rafts, J. Biol. Chem. 275 (2000) 2191-2198.

[36] M. Wan, J. Li, K. Herbst, J. Zhang, B. Yu, X. Wu, T. Qiu, W. Lei, C. Lindvall, B.O. Williams, H. Ma, F. Zhang, X. Cao, LRP6 mediates cAMP generation by G protein-coupled receptors through regulating the membrane targeting of Gαs, Sci Signal 4 (2011) ra15.

[37] M. Crouthamel, D. Abankwa, L. Zhang, C. DiLizio, DR. Manning, J.F. Hancock, P.B. Wedegaertner, An N-terminal polybasic motif of Gαq is required for signaling and influences membrane nanodomain distribution, Mol. Pharmacol.78 (2010) 767-777.

[38] G. Vereb, J. Szollosi, J. Matko, P. Nagy, T. Farkas, L. Vigh, L. Matyus, T.A. Waldmann, S. Damjanovich, Dynamic, yet structured: The cell membrane three decades after the Singer-Nicolson model, Proc. Natl. Acad. Sci. U.S.A. 100 (2003) 8053-8058.

[39] P.V. Escribá, P.B. Wedegaertner, F.M. Goñi, O. Vögler, Lipid-protein interactions in GPCR-associated signaling, Biochim. Biophys. Acta 1768 (2007) 836-852.

[40] O. Rocks, M. Gerauer, N. Vartak, S. Koch, Z. Huang, M. Pechlivanis, J. Kuhlmann, L. Brunsveld, A. Chandra, B. Ellinger, H. Waldmann, P.I.H. Bastiaens, The palmitoylation machinery is a spatially organizing system for peripheral membrane proteins, Cell 141 (2010) 458-471.

[41] J. Novotny, D. Durchankova, R.J. Ward, J.J. Carrillo, P. Svoboda, G. Milligan, Functional interactions between the alpha 1b-adrenoceptor and Galpha11 are compromised by de-palmitoylation of the G protein but not of the receptor, Cell signal. 18 (2006) 1244-1251.

[42] P.V. Escriba, M. Sastre, J.A. Garcia-Sevilla, Disruption of cellular signaling pathways by daunomycin through destabilization of nonlamellar membrane structures, Proc. Natl. Acad. Sci. U.S.A. 92 (1995) 7595-7599.

[43] L. Busconi, P.M. Boutin, B.M. Denker, N-terminal binding domain of Galpha subunits: involvement of amino acids 11-14 of Galphao in membrane attachment, Biochem. J. 323 (1997) 239-244.

[44] L. Busconi, B.M. Denker, Analysis of the N-terminal binding domain of Go alpha, Biochem. J. 328 (1997) 23-31.

[45] K.H. Pedone, J.R. Hepler, The importance of N-terminal polycysteine and polybasic sequences for G14alpha and G16alpha palmitoylation, plasma membrane localization, and signaling function, J. Biol. Chem. 282 (2007) 25199-25212.

[46] J. Sot, M. Ibarguren, J.V. Busto, L.R. Montes, F.M. Goñi, A. Alonso, Cholesterol displacement by ceramide in sphingomyelin-containing liquid-ordered domains, and generation of gel regions in giant lipidic vesicles, FEBS Lett. 582 (2008) 3230-3236.

[47] K. Simons, E. Ikonen, Functional rafts in cell membranes, Nature 387 (1997) 569-572.

[48] K.A. Melkonian, A.G. Ostermeyer, J.Z. Chen, M.G. Roth, D.A. Brown, Role of lipid modifications in targeting proteins to detergent-resistant membrane rafts. Many raft proteins are acylated, while few are prenylated, J. Biol. Chem. 274 (1999) 3910-3917.

[49] P.V. Escribá, P.B. Wedegaertner, F.M. Goñi, O. Vögler. Lipid-protein interactions in GPCR-associated signaling. Biochim. Biophys. Acta 1768 (2007) 836-852.

[50] R.M. Peitzsch, S. McLaughlin, Binding of acylated peptides and fatty acids to phospholipid vesicles: pertinence to myristoylated proteins, Biochemistry 32 (1993) 10436-10443.

[51] J. Morales, C.S. Fishburn, P.T. Wilson, H.R. Bourne, Plasma membrane localization of G alpha z requires two signals, Mol. Biol. Cell 9 (1998) 1-14.

[52] C.S. Fishburn, S.K. Pollitt, H.R. Bourne, Localization of a peripheral membrane protein: Gbetagamma targets Galpha(Z), Proc. Natl. Acad. Sci. U.S.A. 97 (2000) 1085-1090.

[53] L. Go, J. Mitchell, Palmitoylation is required for membrane association of activated but not inactive invertebrate visual Gqα, Comp. Biochem. Physiol. *B* 135 (2003) 601-609.

[54] S.M. Pontier, Y. Percherancier, S. Galandrin, A. Breit, C. Galés, M. Bouvier, Cholesterol-dependent separation of the β2-adrenergic receptor from its partners determines signaling efficacy, J. Biol. Chem. 283 (2008) 24659-24672.

[55] V.O. Rybin, X. Xu, M.P. Lisanti, S.F. Steinberg, Differential targeting of beta-adrenergic receptor subtypes and adenylyl cyclase to cardiomyocyte caveolae. A mechanism to functionally regulate the cAMP signaling pathway, J. Biol. Chem. 275 (2000) 41447-41457.

[56] S. Terés, V. Lladó, M. Higuera, G. Barceló-Coblijn, M.L. Martin, M.A. Noguera-Salvà, A. Marcilla-Etxenike, J.M. García-Verdugo, M. Soriano-Navarro, C. Saus, U. Gómez-Pinedo, X. Busquets, P.V. Escribá, 2-Hydroxyoleate, a nontoxic membrane binding anticancer drug, induces glioma cell differentiation and autophagy, Proc. Natl. Acad. Sci. U.S.A. 109 (2012) 8489-8494.

[57] D. Abankwa, H. Vogel, A FRET map of membrane anchors suggests distinct microdomains of heterotrimeric G proteins, J Cell Sci 120 (2007) 2953-2962.

[58] G.L. Nicolson, M.E. Ash, Lipid replacement therapy: A natural medicine approach to replacing damaged lipids in cellular membranes and organelles and restoring function, *Biochim. Biophys. Acta.* 1838 (2014) 1657-1679.

[59] J.B. Hurley, M.I. Simon, D.B. Teplow, J.D. Robishaw, A.G. Gilman, Homologies between signal transducing G proteins and ras gene products, Science 226 (1984) 860-862.

FIGURE LEGENDS

Figure 1. Lipid characterization of Gαi$_1$ proteins. **(A)** Inhibition of myristoylation (HMA+) caused an electrophoretic mobility shift for the *WT* and *Pal*$^-$ Gαi$_1$ proteins to apparently higher molecular weights. The immunoreactive bands corresponding to non-myristoylated and myristoylated proteins are indicated as 'a' and 'b' respectively in the different panels. A third immunoreactive band ('c') appears to be smaller in the figure and it may correspond to a proteolytic fragment of Gαi$_1$ [59]. Inhibition of palmitoylation (FPA+) did not alter the mobility of the *WT* Gαi$_1$ protein. The *Myr*$^-$ Gαi$_1$ protein mutant, which lacks both myristic and palmitic acids (and therefore could also abbreviated as *Myr*$^-$ *Pal*$^-$), had an electrophoretic mobility identical to that of the non-myristoylated *Pal*$^-$ and *WT* Gαi$_1$ proteins. M, molecular weight marker. **(B)** Lipid characterization of purified Gαi$_1$ proteins**.** *Upper panel*, the electrophoretic mobility of *Myr*$^-$ (i.e., *Myr*$^-$ *Pal*$^-$), *Pal*$^-$ and *WT* Gαi$_1$ proteins (124 ng, 100 ng and 112 ng, respectively) purified from the cytosolic fraction ('*Cyt.*') was compared with that of the myristoylated (HMA-) and non-myristoylated (HMA+) standards obtained from the assays of myristoylation inhibition. *Lower panel*, the electrophoretic mobility of the *WT* Gαi$_1$ protein purified from total membranes was compared with that of a standard, as indicated above. The two bands of purified *WT* Gαi$_1$ protein (7 and 22 ng, from left to right) correspond to fully myristoylated proteins ('b'). **(C)** autoacylation of Gαi$_1$ protein. Palmitoylation of *WT* and *Pal*$^-$ Gαi$_1$ proteins was analyzed by acyl-biotinyl exchange. *Upper panel*, the intense band corresponding to *Pal*$^+$ *WT* Gαi$_1$ and the absence of a signal associated with *Pal*$^-$ Gαi$_1$ shows that only *Pal*$^+$ *WT* Gαi$_1$ incorporated palmitic acid. Biotinylated Gαi$_1$ protein ('Gα$^{\phi}$') was detected with IRDye-conjugated streptavidin (excitation peak at 680 nm). *Lower panel*, identical amounts of *Pal*$^-$ Gαi$_1$ and *Pal*$^+$ Gαi$_1$ proteins were loaded (120 ng). The detection of the total Gαi$_1$ protein (indicated as 'Gα$^{\phi\phi}$') was carried out using a monoclonal antibody against Gαi$_1$ and an IRDye-conjugated anti-mouse IgG (excitation peak at 780 nm). Gαi$_1$ protein standards *st-1* (54 ng), *st-2* (87 ng) and *st-3* (110 ng) were used for quantification.

Figure 2. Effect of PE on the binding of Gαi$_1$ to model membranes. (**A**) Binding of Gαi$_1$ proteins to model membranes with increasing PE content (protein bound relative to the total Gαi$_1$ protein) in function of their acylation status. (**B**) Binding of *Pal*$^+$ and *WT* Gαi$_1$ proteins to lipid vesicles containing PE and to PC membranes. (**C**) Binding of *Pal*$^-$ and *Myr*$^-$ (i.e., *Myr*$^-$ *Pal*$^-$) Gαi$_1$ proteins to lipid vesicles containing PE and to PC membranes. In (**B**) and (**C**) the binding to PC membranes was taken as the reference (100%). Representative

immunoblots from binding experiments are shown. The data represent the mean ± S.E.M from 3-8 independent experiments.

Figure 3. Effect of PS on the binding of Gαi$_1$ to model membranes. (**A**) Binding of Gαi$_1$ proteins to model membranes with different PS content as a function of their acylation status (protein bound relative to the total Gαi$_1$ protein). (**B**) Binding of *Pal*$^+$, *Pal*$^-$ and *Myr*$^-$ (i.e., *Myr*$^-$ *Pal*$^-$) Gαi$_1$ proteins to lipid vesicles containing increasing amounts of PS, with binding to PC taken as the reference (100%). Representative immunoblots of each binding experiment are also shown and the data represents the mean ± S.E.M from 3-8 independent experiments: ***, $p < 0.001$; **, $p < 0.01$; *, $p < 0.05$; '#' indicates significant differences in the binding of *Myr*$^-$ (i.e., *Myr*$^-$ *Pal*$^-$) Gαi$_1$ to LUVs with respect to *WT* and *Pal*$^-$ Gαi$_1$ proteins.

Figure 4 Binding of Gαi$_1$ protein to lamellar-prone membranes. Binding of Gαi$_1$ proteins with different degrees of acylation to lamellar-prone PC and PC:PE:CHO:SM (raft-like, L_o) membranes. The bars correspond to the mean ± S.E.M from 4-7 independent experiments: ***, $p < 0.001$; **, $p < 0.01$, *; $p < 0.05$.

Figure 5. Binding of recombinant Gαi$_1$ proteins to Sf9 cell membranes. The binding of each recombinant Gαi$_1$ protein produced in Sf9 cells is shown. Immunoblots illustrate the distribution of the different Gαi$_1$ proteins between the cell membrane (P, pellet) and the cytosolic (SN, supernatant) fraction in these experiments. The results shown are the mean ± S.E.M from 3 independent experiments: ***, $p < 0.001$; **, $p < 0.01$; *, $p < 0.05$; '#' indicates significant differences in the binding of *Myr*$^-$ (i.e., *Myr*$^-$ *Pal*$^-$) Gαi$_1$ to Sf9 membranes with respect to *Pal*$^-$ Gαi$_1$ protein.

Figure 6. Effect of palmitoylation on the secondary structure of Gαi$_1$ protein. (**A**) Predicted α helical structure of the N-terminus of the Gαi$_1$ protein. (**B**) Multiple alignment of the N-terminal sequence of the different rat myristoylated Gα proteins. Positively charged conserved residues are highlighted in bold face. (**C**) Helical wheel projection of residues 7-39 of the Gαi$_1$ protein. The helical Gαi$_1$ protein projection shows the relative volume occupied by the different amino acids in the helix and their relative position. Conserved basic amino acids specifically map to one side of the structure. The hydrophobic moment of this helix is depicted as an arrow in the centre of the projection. The position of the peptide with respect to the membrane for the myristoylated (M, solid line) and double acylated (M, P, dotted line)

peptide is shown with an arrow. The inset depicts these relative positions with respect to the membrane interface of the charged amino acids for the double acylated (left) or only myristoylated (right) Gαi$_1$ protein. Negatively charged phospholipids are shown in blue and uncharged (zwitterionic) phospholipids in red (**D**) A comparison of the stable structures that correspond to the non-acylated and acylated peptides that contain the five N-terminal amino acids of Gαi$_1$. The structure of this region when both myristic and palmitic acids are present is shown in yellow, whereas the N-terminal region containing only myristic acid is shown in black and the non-acylated peptide is shown in red. Myristic acid is indicated as 'M' and palmitic acid as 'P' in the different panels. Arrows show the most relevant changes in the relative position of atoms as a consequence of N-terminal lipidation.

TABLES

Table 1

Amino acid sequence of the recombinant wild type Gαi$_1$ protein.

H_2N- GCTLSAEDKAAVERSKMIDRNLREDGEKAAREVKLLLLGAGESGKSTIVKQMKI
IHEAGYSEEECKQYKAVVYSNTIQSIIAIIRAMGRLKIDFGDAARADDARQLFVLAGAAE
EGFMTA∗**GGHHHHHHGGGMTA**ELAGVIKRLWKDSGVQACFNRSREYQLNDSAAYY
LNDLDRIAQPNYIPTQQDVLRTRVKTTGIVETHFTFKDLHFKMFDVGGQRSERKKWIHC
FEGVTAIIFCVALSDYDLVLAEDEEMNRMHESMKLFDSICNNKWFTDTSIILFLNKKDLF
EEKIKKSPLTICYPEYAGSNTYEEAAAYIQCQFEDLNKRKDTKEIYTHFTCATDTKNVQF
VFDAVTDVIIKNNLKDCGLF-COOH

∗ 6 x His tag inserted at position 121 of Gαi$_1$ (highlighted in bold face).

Table 2

PCR primers used and their corresponding amino acid sequences.

Gαi$_1$ subunit	Forward oligonucleotides	N-terminal sequence
	*Eco*RI CDS X	
wild-type Gαi$_1$	5´-ATCGAATTCATGGGCTGCACGCTGAGCGCC-3’	M G **C** T L S A E D*
	5´-ATCGAATTC 5XXXXXXXXX	
Myr$^-$ (*Pal*) Gαi$_1$	5´ATCGAATTCATGGCCTGCACGCTGAGCGCC-3’	M A **C** T L S A E D
	5´- 5XXXXXXXXXXXXX	
Pal$^-$ Gαi$_1$	5´-ATCGAATTCATGGGCTCCACGCTGAGCGCC-3’	M G S T L S A E D

Reverse oligonucleotide
5XXXXXXXXXXXXX
*Not*I CDS N
5´-CTGGCGGCCGCTTAAAAGAGACCACAATCT-3´

The sequences shown correspond to the amino acids present in the N-terminal region of the protein after PCR amplification with the primers indicated on the left. The underlined G corresponds to the myristoylation site, while the palmitoylation site C is shown in bold face.

FIGURES

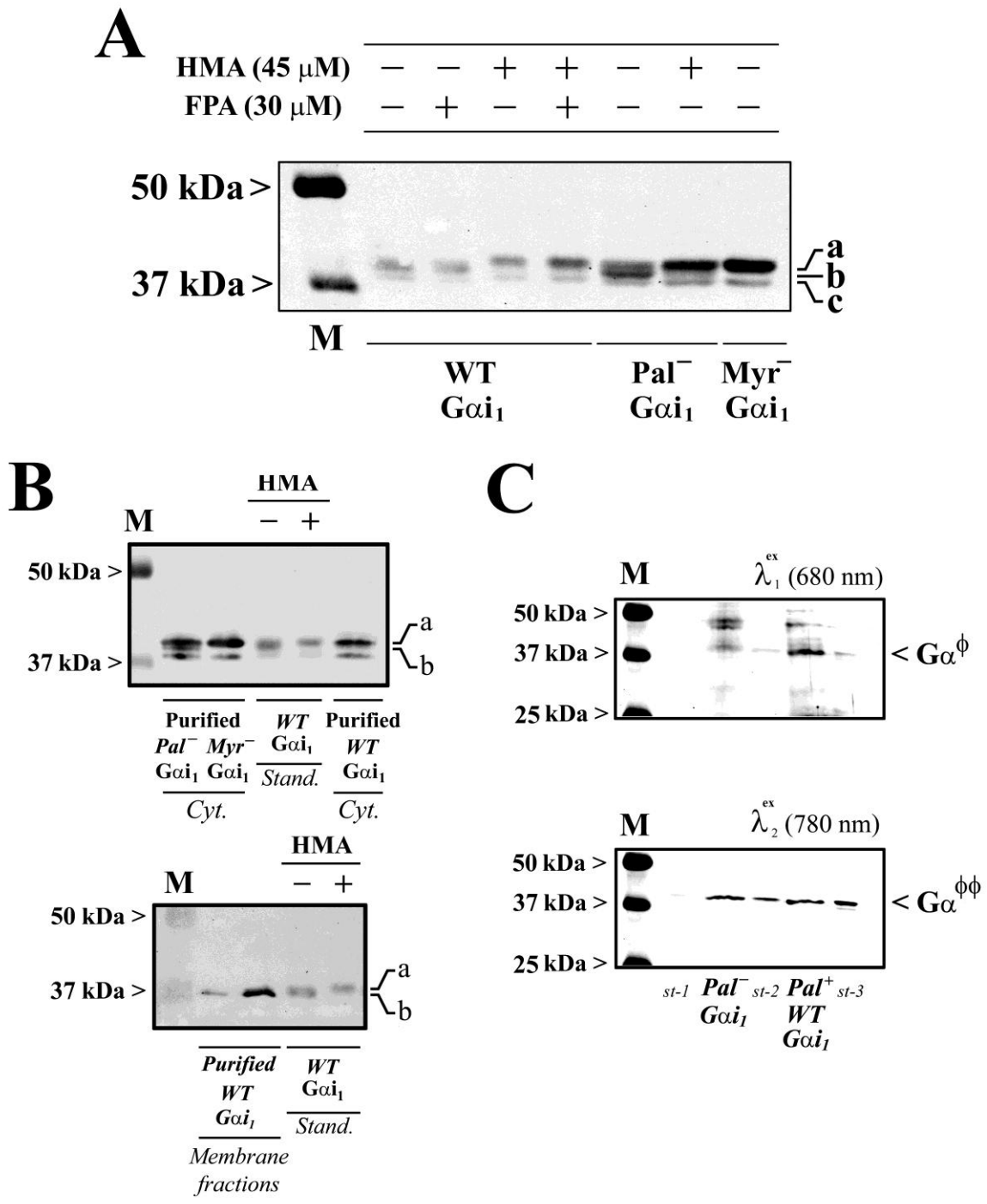

Figure 1

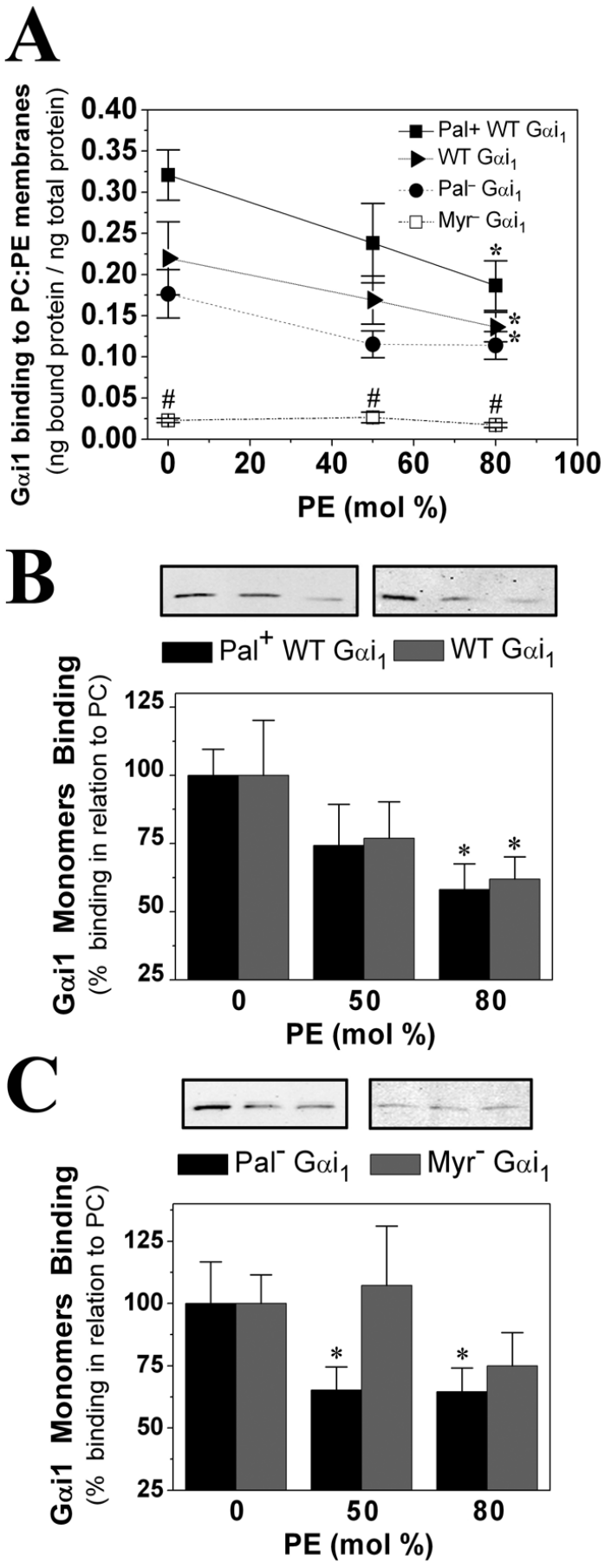

Figure 2

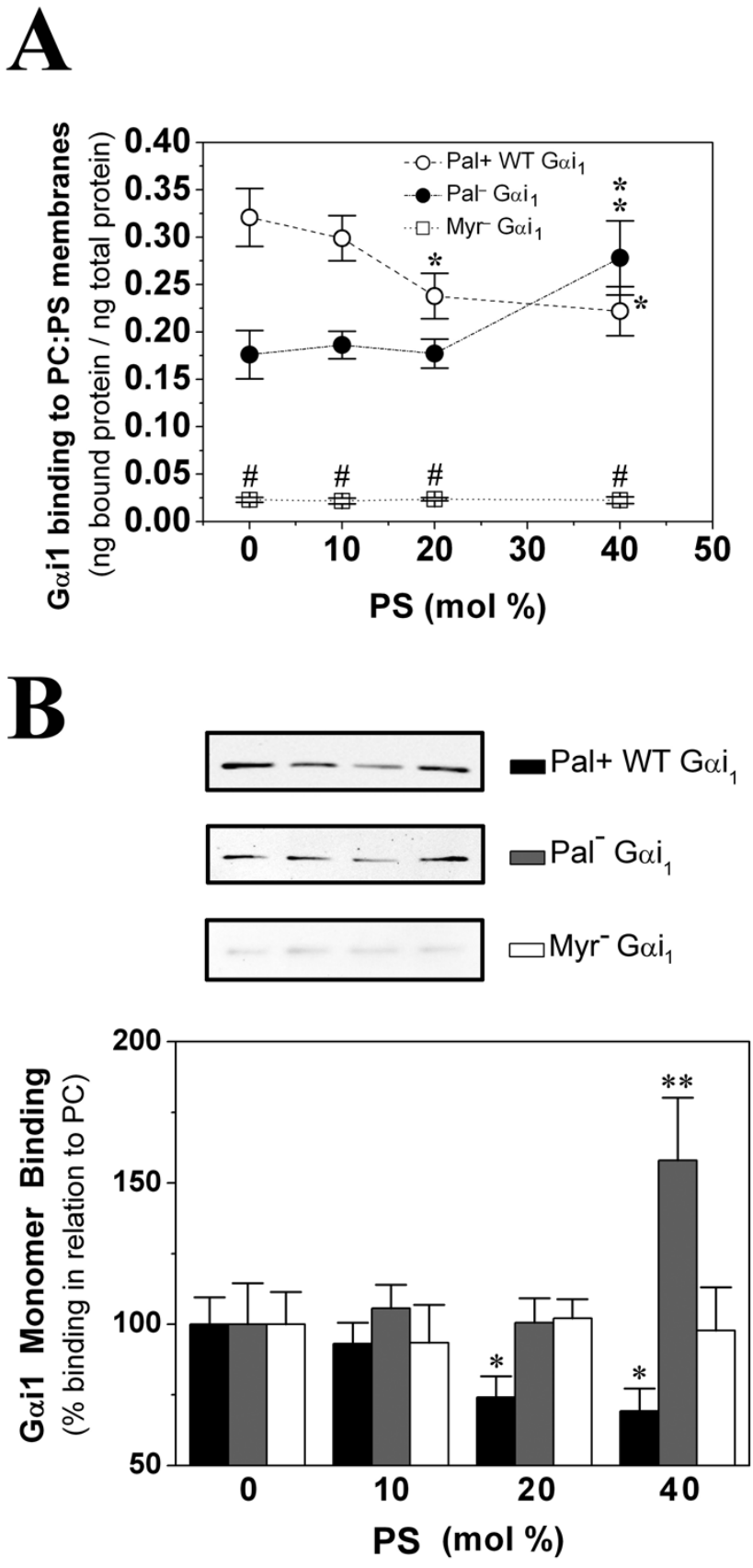

Figure 3

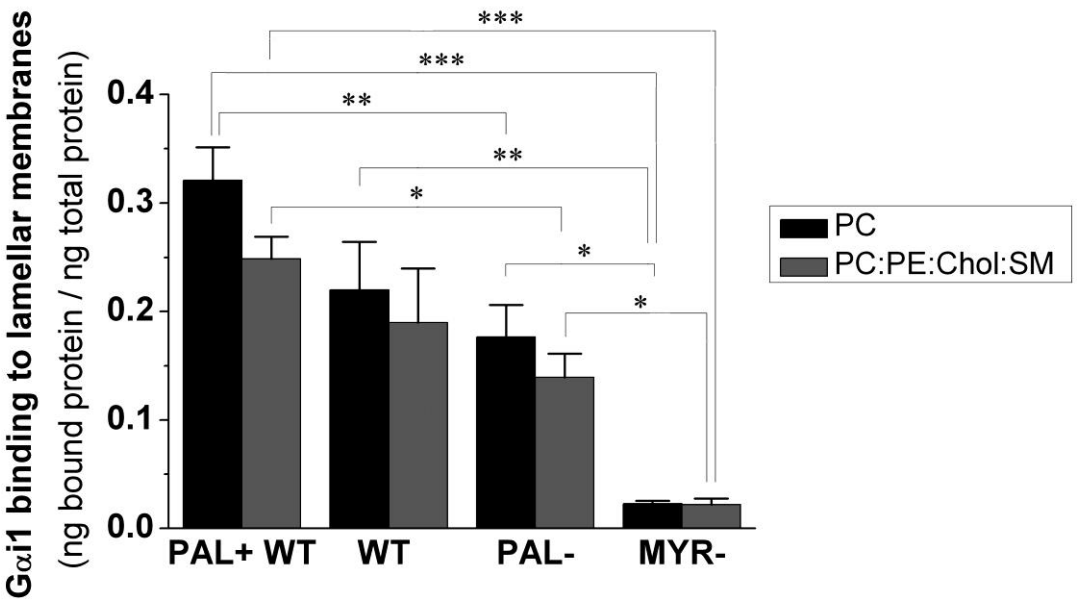

Figure 4

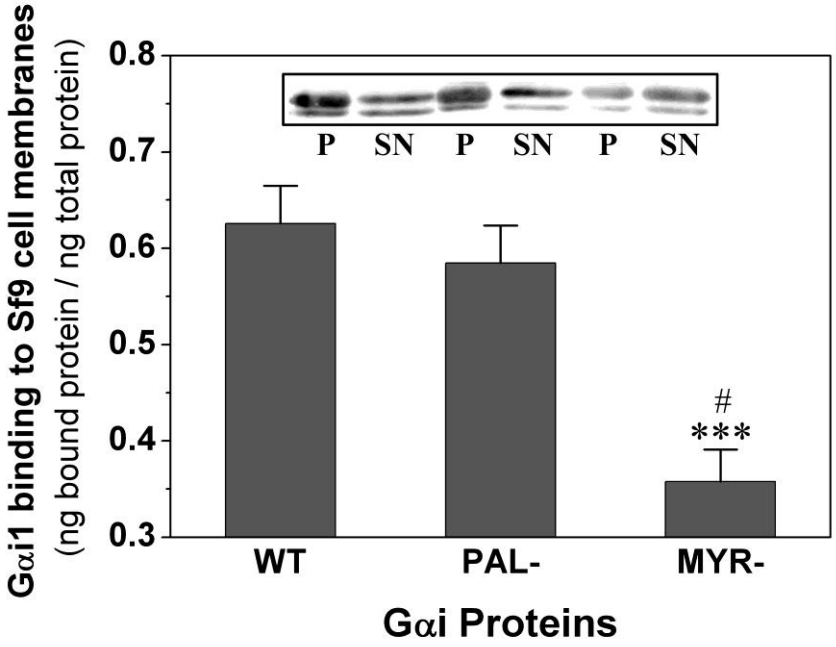

Figure 5

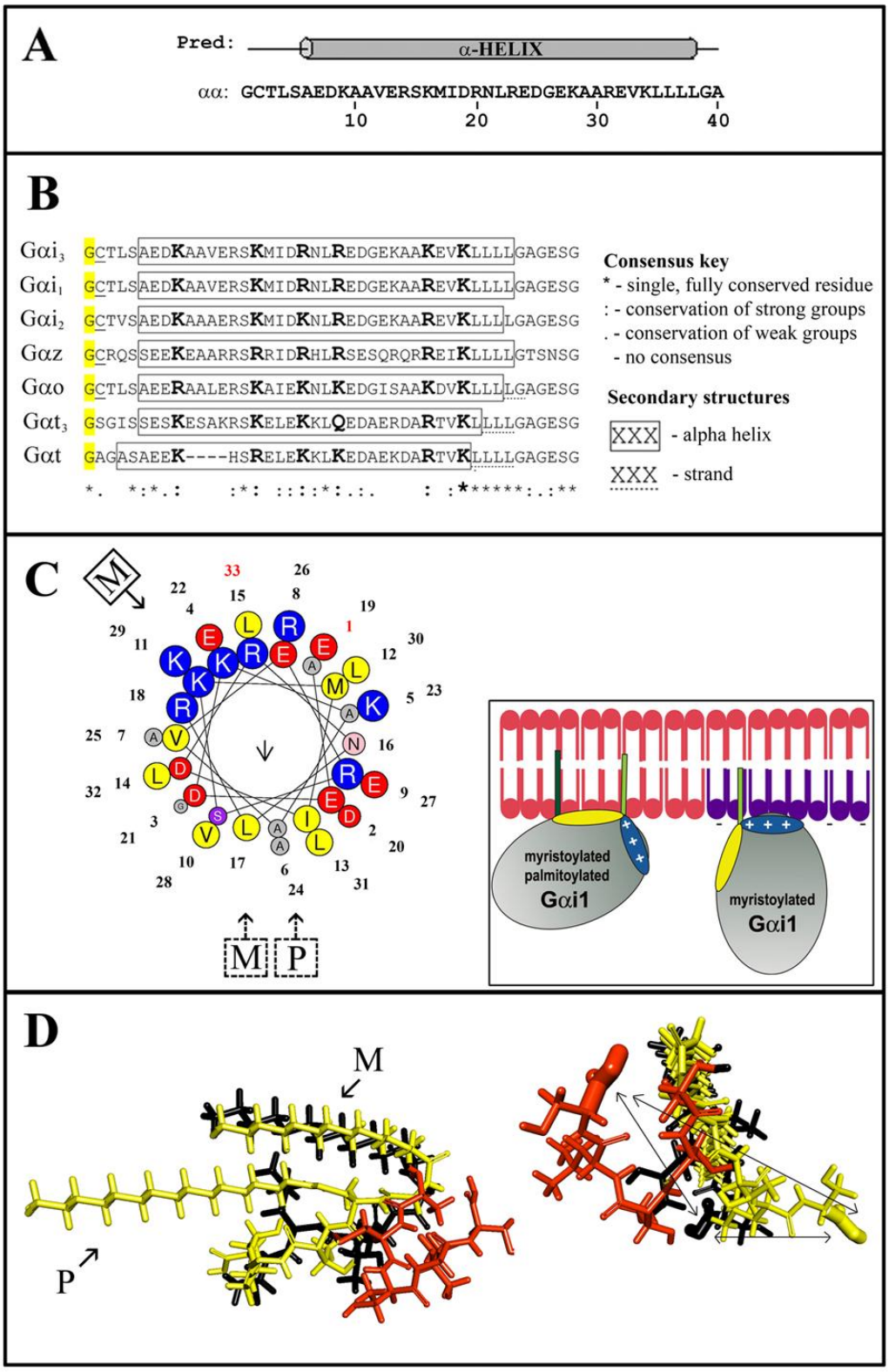

Figure 6

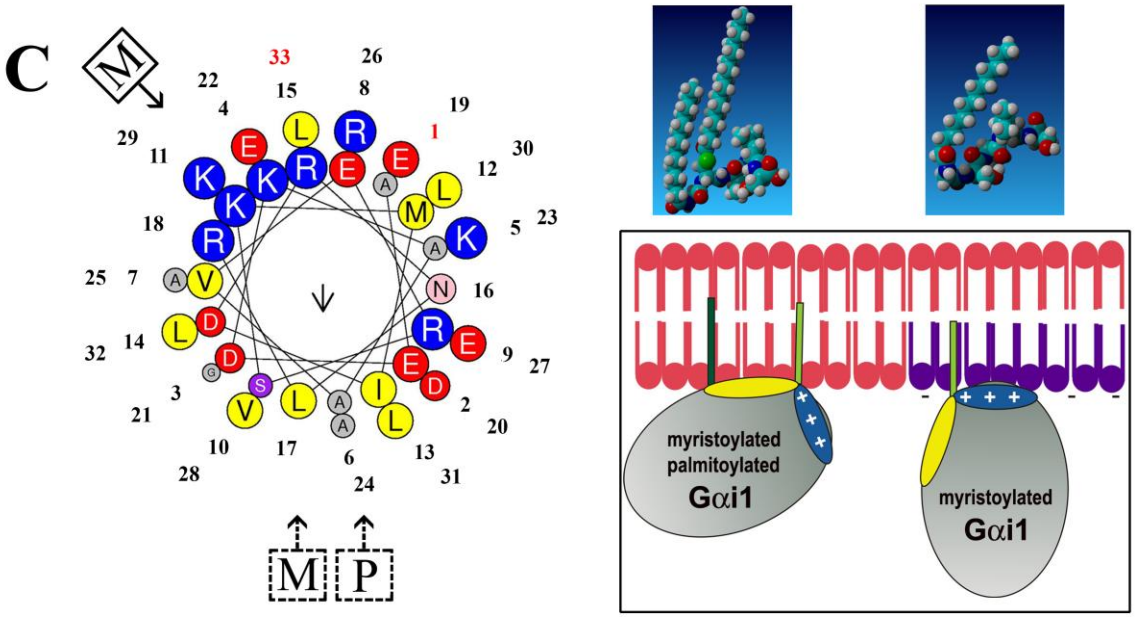

Graphical abstract

Highlights

1. The Gαi$_1$ protein has a permanent myristoyl and a reversible palmitoyl moiety
2. Myristoyl and palmitoyl moieties regulate Gαi$_1$ membrane microdomain localization
3. Myristoylation favors Gαi$_1$ protein localization to ordered lamellar membranes
4. Gαi$_1$ palmitoylation increases its affinity to lamellar domains with negative charge
5. Palmitoylation induces Gαi$_1$ basic amino acid exposure to the membrane surface